Sains Malaysiana 52(8)(2023): 2191-2207
http://doi.org/10.17576/jsm-2023-5208-03

Removal Efficiency for Micro-Polystyrene in Water by the Oil-Based Ferrofluid Employ Response Surface Methodology

(Keberkesanan Penyingkiran Mikro-Polisterina dalam Air oleh Bendalir Magnetik Berasaskan Minyak menggunakan Kaedah Gerak Balas Permukaan)

Natasha Nizam[1], Sumithra Mohanasunthar[1], Alyza A. Azmi[1], Sabiqah Tuan Anuar[1], Yusof Shuaib Ibrahim[1] & Wan Mohd Afiq Wan Mohd Khalik[1,2,*]

[1]*Microplastic Research Interest Group, Faculty of Science and Marine Environment, Universiti Malaysia Terengganu, 21030 Kuala Nerus, Terengganu, Malaysia*
[2]*Water Analysis Research Centre, Faculty of Science and Technology, Universiti Kebangsaan Malaysia, 43600 UKM Bangi, Selangor, Malaysia*

Received: 15 February 2023/Accepted: 12 July 2023

ABSTRACT

This research article presents a study on the potential use of oil-based ferrofluid for the efficient removal of microplastics from water. The targeted analyte, micro-polystyrene (micro-PS), was chosen along with palm oil as the carrier liquid. Fourier Transform Infrared (FTIR) analysis was conducted to identify the main peaks in the ferrofluid, including carboxyl group (1542 cm^{-1}), C-H bonding (1022 cm^{-1}), CH_2 bonding (2941 cm^{-1}), CH_3 bonding (3461 cm^{-1}), C=C bonding (1255 cm^{-1}), and Fe-O (597.34 cm^{-1}). A comprehensive investigation of the synergistic effect of six variables was performed: volume of oil (4-15 mL), weight of magnetite nanoparticles (0.1-0.2 g), stirring rate (132-468 rpm), contact time (3-12 min), pH value of water samples (pH 6-8), and effect on ionic strength (0-16 g/L). Response surface methodology, including 2^6-Plackett-Burman and 2^4-central composite design, were employed to establish the relationship between the variables. The optimum operational settings proposed by the model were as follows: volume of oil (14.6 mL), weight of magnetite nanoparticles (0.1 g), stirring rate (216 rpm), contact time (3.29 min), pH value of water samples (pH 6-6.5), and effect on ionic strength (16 g/L), resulting in a remarkable removal efficiency of 91.09 ± 0.99%. The method exhibited desirable figures of merit, including a low bias (%RSD) of below 5% and the ability to reuse the ferrofluids for up to five cycles. Additionally, an analytical greenness metric was employed to assess the environmental impact of the sample preparation process, with a green score of 0.69/1.0 (indicating a light green colour). Future work in this field could focus on the scalability of the developed method and its applicability to real-wastewater treatment.

Keywords: Emerging contaminant; magnetic separation; marine debris; microplastic

ABSTRAK

Artikel penyelidikan ini membincangkan satu kajian mengenai kegunaan berpotensi bendalir magnetik berasaskan minyak untuk penyingkiran yang berkesan bagi mikroplastik daripada air. Analit sasaran, mikro-polisterena (mikro-PS), dipilih bersama dengan minyak kelapa sawit sebagai cecair pembawa. Analisis Transformasi Fourier Inframerah (FTIR) telah dijalankan untuk mengenal pasti puncak-puncak utama dalam bendalir magnetik, termasuk kumpulan karboksil (1542 cm^{-1}), ikatan C-H (1022 cm^{-1}), ikatan CH_2 (2941 cm^{-1}), ikatan CH_3 (3461 cm^{-1}), ikatan C=C (1255 cm^{-1}) dan Fe-O (597.34 cm^{-1}). Kajian menyeluruh tentang kesan sinergi enam pemboleh ubah telah dijalankan: isi padu minyak (4-15 mL), berat nanozarah magnetit (0.1-0.2 g), kadar pengacuan (132-468 rpm), masa sentuhan (3-12 min), nilai pH sampel air (pH 6-8) dan kesan ke atas kekuatan ion (0-16 g/L). Kaedah gerak balas permukaan, termasuk 2^6-Plackett-Burman dan 2^4-reka bentuk komposit pusat digunakan untuk menetapkan hubungan antara pemboleh ubah tersebut. Tetapan operasi optimum yang dicadangkan oleh model adalah seperti berikut: isi padu minyak (14.6 mL), berat nanozarah magnetit (0.1 g), kadar pengacuan (216 rpm), masa sentuhan (3.29 min), nilai pH sampel air (pH 6-6.5) dan kesan ke atas kekuatan ion (16 g/L) yang menghasilkan kecekapan penyingkiran yang baik pada tahap 91.09 ± 0.99%. Kaedah ini menunjukkan ciri prestasi yang diingini, termasuk kebolehan untuk digunakan semula hingga lima kitar bagi bendalir magnetik dan ralat rendah (%RSD) di bawah 5%. Tambahan pula, satu metrik kelestarian analitik digunakan untuk menilai impak alam sekitar proses penyediaan sampel dengan skor kelestarian 0.69/1.0 (mewakili warna hijau muda). Penyelidikan masa depan dalam bidang ini boleh memberi tumpuan kepada skalabiliti kaedah yang dibangunkan dan kebolehgunaannya dalam rawatan air sisa sebenar.

Kata kunci: Bahan pencemar baharu muncul; mikroplastik; pemisahan magnetik; serpihan sampah

Introduction

The research on microplastic removal techniques has garnered significant attention from scientists and researchers. Microplastics have been identified as excellent carriers of toxic organic chemicals due to their large specific surface area and strong hydrophobic nature. This specific surface area plays a crucial role in their ability to adsorb pollutants, transfer them to organisms, and support microbial growth (Amelia et al. 2021; Ma et al. 2019). Understanding the negative consequences of microplastic presence in water, numerous approaches have been proposed by researchers, including physical methods such as coagulation, agglomeration, sorption, filtration, and membrane processes, as well as chemical methods like photocatalytic degradation, and biological methods involving bacteria or microorganism degradation (Liu et al. 2019; Ma et al. 2019; Poerio, Piacentini & Mazzei 2019; Tofa et al. 2019).

The efficacy of physical-based removal processes can be influenced by the interaction between coagulants and the surface of virgin plastics. In the case of aged plastics, surface interactions are likely to increase following photooxidation and fragmentation, but may require additional steps for effective removal. Chemical methods have shown promising efficiency in laboratory-scale testing, but their practical application in real treatment scenarios needs to consider cost, chemical usage, and energy consumption. Biological treatment, although regarded as a promising technology, often exhibits slow degradation rates, instability, and may even generate secondary pollutants (Lapointe et al. 2020; Rajala et al. 2020; Shi et al. 2022). Considering microplastics as primarily physical pollutants, trapping methods in aqueous systems appear to be effective without introducing new complications.

Water samples have been found to contain various types of plastic, including polyethylene, polypropylene, polyvinyl chloride, and polystyrene. Polystyrene (PS) stands out as one of the most extensively used commercial plastics globally. It is a polymer derived from styrene monomers, characterized by the presence of a benzene aromatic group and a specific gravity ranging from 1.04 g/cm^3 to 1.07 g/cm^3. This polymer has been frequently detected in air (Peñalver et al. 2021), marine waters (Khalik et al. 2018), rivers (Choong et al. 2021; Ma et al. 2022), sediments (Li et al. 2020), and various other environments. Due to its density being similar to that of water, low-buoyancy PS particles can easily remain suspended or float in water, posing a higher risk compared to plastics that settle during drinking water treatment processes.

The presence of PS has been found to have detrimental effects on organisms, including reduced chlorophyll concentration in algae, impaired oyster reproductive functionality, decreased metabolic activity, oxidative stress, and disrupted blood circulation in organisms such as fish (Deng et al. 2017; Issac & Kandasubramanian 2021; Sun et al. 2019). When exposed to the environment, PS can undergo oxidation and cracking processes, resulting in reduced sorption capacity for organic compounds compared to pristine particles (Hüffer, Weniger & Hofmann 2018). Therefore, by focusing on PS as the targeted analyte, this study aims to address the specific challenges and risks associated with this widely distributed microplastic pollutant, contributing to a better understanding of its removal and mitigation in water environments.

With growing concerns over the abundance of microplastics in the environment, researchers are actively seeking to design low-cost yet effective removal procedures. Some of the techniques being explored include harnessing biochar, membrane filtration, and the utilization of ferrofluids (Pizzichetti et al. 2021; Pramanik, Pramanik & Monira 2021; Siipola et al. 2020). Ferrofluids, in particular, are magnetic liquids consisting of stable colloidal suspensions containing dispersed metal nanoparticles in a liquid medium, such as oil, organic solvents, or water (Wang et al. 2022). The rheological properties of ferrofluids are influenced by various factors, including shear conditions (such as magnetic field strength, magnetic field direction, shear rate, and temperature) as well as the properties of nanoparticles and carrier liquids (such as nanoparticle concentration, average particle size, particle size distribution, type of base liquid, and types of nanoparticles), which are continuously being improved and optimized (Chen et al. 2021).

Literature proposes various synthesis procedures for ferrofluids, including co-precipitation, de-collide, electrophoresis, grinding, and thermal decomposition, with co-precipitation being widely used due to its simplicity (Li & Li 2021). Ferrofluids offer several advantages, such as good dispersibility, rapid removal of pollutants, and reusability (Nayebi & Shemirani 2021). They have been successfully employed in the removal of pollutants like metals (Davudabadi Farahani et al. 2015; Kadakia 2012) as well as microplastics (Hamzah et al. 2021).

Oil-based ferrofluids are versatile colloidal suspensions consisting of magnetic nanoparticles dispersed in carrier liquids, which can include mineral oil, silicone oil, vegetable oils, or synthetic oils. The

choice of carrier liquid depends on specific requirements and considerations. For instance, mineral oil is often preferred due to its good wetting properties and its ability to prevent the agglomeration of magnetic nanoparticles (Joseph & Mathew 2014). On the other hand, vegetable oils offer the advantage of being renewable and biodegradable, making them more environmentally friendly options (Nabeel Rashin, Kutty & Hemalatha 2014). However, additional modifications may be necessary to enhance stability and performance when using vegetable oils as carrier liquids. These oil-based ferrofluids find applications in various fields, such as pollutant removal, biomedicine, and engineering. Despite their potential, challenges remain in optimizing their rheological properties, developing efficient nanoparticle synthesis techniques, and ensuring long-term stability for practical applications (Oehlsen et al. 2022). In microplastic removal systems, when ferrofluids are introduced to a microplastic suspension, hydrophobic microplastics adsorb the hydrophobic oils, resulting in the formation of microplastic-oil-magnetite complexes, which can be easily extracted using a magnet (Henriques 2022; Yap & Tan 2021).

This research aims to propose an experimental condition for efficient micro-PS removal using an oil-based ferrofluid, employing the powerful technique of response surface methodology (RSM). RSM is known for its ability to optimize complex processes and systems by efficiently exploring the design space and identifying optimal conditions. Compared to the traditional one-factor-at-a-time approach, RSM significantly reduces the number of experiments required. By generating response surface models, researchers can predict the response variable at different combinations of variables, enabling the determination of optimal levels that lead to the desired removal efficiency (Bezerra et al. 2008; Hanrahan & Lu 2006). The ferrofluids were synthesized using a direct dispersion method, and their characterization was thoroughly conducted. Factors controlling the removal rate were carefully studied to elucidate the synergistic and antagonistic impacts within the identified optimum conditions. Furthermore, the proposed method's environmental impact was evaluated by utilizing the analytical greenness metric (AGREEprep) to assess its adherence to green criteria in sample preparation.

Materials and Methods

Reagent and Apparatus

Palm oil, corn oil, canola oil, and sunflower seed oil weighing approximately 0.5 kg to 1.0 kg were obtained from a local market. To ensure consistency, a new batch of micro-PS with sizes ranging from 2 mm to 4 mm was purchased from Isthome trading in Kedah, Malaysia, with a total weight of 1 kg. Iron (II, III) in the form of $FeCl_2{\cdot}_4H_2O$ and $FeCl_3{\cdot}_6H_2O$ was sourced from Sigma-Aldrich (Steinheim, Germany). Neodymium magnet bars measuring 100 mm in length, 10 mm in width, and 5 mm in thickness, as well as magnet rods, were purchased from Magnut, Malaysia. Additionally, stainless steel ESD-15 tweezers were acquired from Techmakers in Malaysia to facilitate the experimental procedures.

Synthesis of Magnetite and Preparation of Ferrofluid

Magnetite nanoparticles were synthesized using the co-precipitation method. A mixture of $FeCl_3{\cdot}_6H_2O$ and $FeCl_2{\cdot}_4H_2O$ in a 2:1 ratio was dissolved in 100 mL of distilled water. The solution was then heated to 80 °C and stirred gently for 10 min. Gradually, 20 mL of NH_4OH was added to the solution while maintaining a controlled stirring speed of 300 rpm. The resulting precipitate of magnetite nanoparticles was separated from the liquid phase using a neodymium magnet bar. The collected precipitate was subsequently dried in an oven at 80 °C for 1 h. This procedure was repeated until a sufficient quantity of magnetite nanoparticles was obtained for the experiment.

Preliminary experiments involved the use of four different plant-based oils, namely palm oil, corn oil, canola oil, and sunflower seed oil. The fabrication of ferrofluids was based on the direct dispersion method, adapted from the method described by Shi, Zhang and Lee (2010) in the literature. In a 100 mL glass beaker, 50 mL of palm oil was added, followed by the introduction of 0.5 g of Fe_3O_4 nanoparticle powder. The mixture was stirred at a low speed of 150 rpm for 10 min, or until the ferrofluid achieved homogeneity. The attainment of homogeneity was indicated by the visual uniformity of the carrier liquid, with no observable agglomeration of Fe_3O_4 nanoparticles. The prepared ferrofluid was then transferred to a 50 mL glass vial and stored at room temperature for subsequent analysis. Similar procedures were applied for the other types of oils.

The characterization of the ferrofluid involved the analysis of its characteristics using ATR-Fourier transformation infrared spectroscopy (Shimadzu Model Nicolet IS20). This technique was employed to identify the main functional groups present in the ferrofluid. Furthermore, the magnetic properties of the formulated ferrofluid were determined using a vibrating sample magnetometer (Lakeshore VSM 7404, USA). The intensity

of the magnetic effervescent tablet was measured under varying applied magnetic fields ranging from -14000 G to 14000 G at room temperature, with a magnetic field strength of 1.40 Tesla. The vibrating sample magnetometer operated at a vibrational frequency of 80 Hz, utilizing a time constant of 3 s to obtain accurate measurements.

SCREENING AND OPTIMIZATION STRATEGY

To minimize the number of experiments required during the optimization stage, screening designs were implemented to assess the main effects of variables. In this study, a 2^6-Plackett Burman design was employed to construct the latent variable in the micro-PS removal procedure. The design matrix for the screening experiment consisted of eight randomly assigned run orders conducted in the laboratory. Each variable was tested at two levels, as indicated in Table 1. The variables under consideration included the volume of oil, weight of magnetite nanoparticles, stirring rate, contact time, pH value of water samples, and the effect of ionic strength. By using this screening design, the impact of each variable on the micro-PS removal process could be efficiently evaluated.

The selection of these specific variables in our study is based on their potential impact on the efficiency of micro-PS removal when using an oil-based ferrofluid. The volume of oil directly affects the quantity of ferrofluid present in the system, which in turn influences the dispersion and coverage of the ferrofluid on the micro-PS particles. The weight of magnetite nanoparticles plays a crucial role as it determines the concentration of magnetic particles within the ferrofluid, thus affecting its magnetic properties and the ability to attract and trap micro-PS. The stirring rate is important as it controls the mixing and agitation of the ferrofluid within the water sample, enabling better contact and interaction between the ferrofluid and micro-PS. The contact time represents the duration of this interaction, with longer contact times allowing for increased adsorption and aggregation of micro-PS by the ferrofluid. The pH of the water sample can impact the surface charge and stability of both the micro-PS particles and the ferrofluid, influencing their interactions. Finally, the ionic strength refers to the concentration of ions in the water sample, which can affect the electrostatic interactions between the ferrofluid and micro-PS. Understanding and optimizing these variables will contribute to improving the overall efficiency of micro-PS removal using oil-based ferrofluid.

Once the latent variables were identified, a 2^4-central composite design was implemented to determine the optimal conditions for the micro-PS removal procedure. The design allowed for the evaluation of curvature by employing a second-order model. The polynomial equation included quadratic terms that helped identify critical points in the process. To assess the fit of the model, analysis of variance (ANOVA) and the coefficient of determination (R^2) were employed. The model with the highest desirability function was selected as the best-fit model for achieving the optimum conditions. This model maximized the capacity of the ferrofluid for the efficient removal of micro-PS.

Data processing and statistical analysis of the percentage removal were conducted using Microsoft Excel 2019, with data sheets specifically prepared for this purpose. The response surface method, which involved the generation of mathematical models to analyze the relationship between variables and the response, was carried out using Statistica 10 (Stat Inc, USA). This software package was utilized to perform all statistical analyses in both the screening and optimization phases of the study, providing comprehensive and reliable results.

REMOVAL PROCEDURE

A 100 mL sample of ultrapure water was carefully transferred into a 250 mL glass beaker. The pH of the water sample was adjusted using either 0.1 N hydrochloric acid or sodium hydroxide solution, according to the values specified in Table 2. To modify the ionic strength, various concentrations of NaCl solution were added. Subsequently, a micro-polystyrene foam weighing 1 g and with a size smaller than 5 mm (as determined through sieving) was added to the beaker and gently stirred using a glass rod. The ferrofluid was then slowly introduced into the water sample. The volume of oil and weight of magnetite nanoparticles were predetermined based on the settings outlined in Table 2. The stirring process was initiated, and the contact time was kept within the predetermined range. Upon completion of the contact time, an external magnet bar was placed on the surface of the ferrofluid to facilitate the retrieval step, as illustrated in Figure 1.

During the micro-PS removal process using oil-based ferrofluid, the ferrofluid was dispersed in the aqueous solution, forming a stable suspension. Subsequently, an external magnetic field was applied to induce magnetization of the nanoparticles in the

ferrofluid, leading to the formation of clusters. These magnetized nanoparticles exhibited an attraction to the micro-PS particles, resulting in the formation of larger agglomerates. To separate the ferrofluid containing the attached microplastics from the rest of the solution, a magnetic separation step was performed using a stronger magnetic field. The recovered ferrofluid, along with the micro-PS agglomerates, underwent further treatment through centrifugation to isolate and properly dispose of the micro-PS particles. The efficiency of the removal process was evaluated based on the volume of oil (indicating reusability) and the weight of the collected micro-PS particles, as quantified by Equation (1).

$$\%\ \text{microPS recovery} = \frac{(\text{weight microPS}) - (\text{weight ferrofluid})}{(\text{initial weight microPS})} \times 100 \quad (1)$$

TABLE 1. Variable study for screening experiment

Variable	Unit	Range
Weight of magnetite nanoparticles	g	1-2
Volume of oil	mL	25-50
Stirring rate	rpm	200-400
Contact time	min	5-10
pH water sample	-	6-8
Effect of ionic strength	g/L	5-15

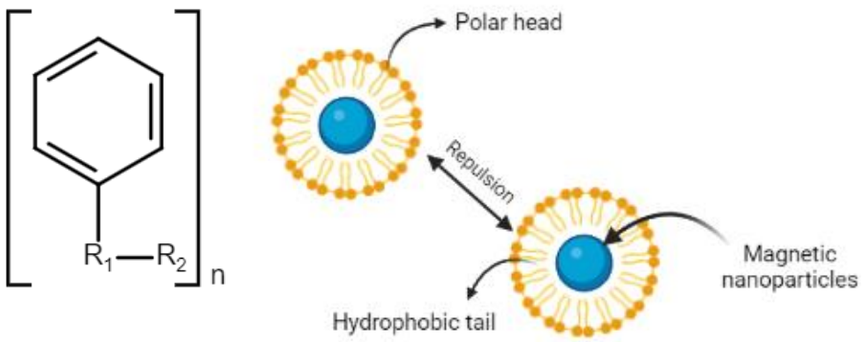

FIGURE 1. Chemical structure of polystyrene (left) and schematic oil based ferrofluid (right)

TABLE 2. Design matrix for screening experiment

Run order	Weight of magnetite nanoparticles (g)	Volume of oil (mL)	Stirring rate (rpm)	Contact time (mins)	pH water sample	Effect of ionic strength (g/L)
1	1	25	200	10	8	15
7	2	50	200	10	6	5
2	1	25	400	10	6	5
5	2	25	200	5	6	15
6	2	25	400	5	8	5
8	2	50	400	10	8	15
4	1	50	400	5	6	15
3	1	50	200	5	8	5

GREENNESS EVALUATION

The greenness criteria of the proposed method were assessed using the AGREEprep® open-source software, available at mostwiedzy.pl/AGREEprep. The evaluation was based on a total score ranging from 0 to 1.0, which took into account 10 impact categories, including solvent selection, material and reagent usage, waste generation, energy consumption, and sample size and throughput. A higher score closer to 1.0 indicated a method with stronger green criteria. To distinguish the significance of each criterion, a weighting system was applied during the assessment, following the approach described by Mušović et al. (2023) and Wojnowski et al. (2022). The results were presented in an easily interpretable colored pictogram, with the inner circle representing the overall sample preparation score, as proposed by Wenzel et al. (2022).

RESULTS AND DISCUSSION

OPTIMAL FERROFLUID SELECTION

The utilization of palm oil as the carrier liquid in the preparation of ferrofluid led to remarkable micro-PS recovery rates exceeding 90% (Figure 2). Palm oil stands out for its notably high viscosity, ranging between 32 mPa.s and 36 mPa.s, surpassing that of alternative liquids commonly employed in similar applications. One crucial factor contributing to the formulation's success was the presence of a stabilizer agent, such as palmitic acid, found naturally in palm oil. According to a study conducted by Gonzalez et al. (2021), the inclusion of a stabilizer agent was reported to play a significant role in facilitating the development of steric repulsions, particularly in the case of ionic surfactants, by introducing ionic repulsion. To prevent undesirable agglomeration, oleic acid, renowned for its surfactant properties, was chosen as the carrier liquid within the palm oil formulation. This decision was based on the intrinsic chemical properties of oleic acid, characterized by the presence of unsaturated π-bonding and alkyl chains, as elucidated by Martinez and Kim (2020). The polar head of the surfactant adhered to the magnetite surface, while the carbonic chain established contact with the oil (Scherer & Figueiredo Neto 2015).

During initial trials, it was observed that an excessive volume of palm oil resulted in an inefficient retrieval process during the post-removal procedure. In response, an additional trial was conducted, wherein the volume of palm oil was reduced. However, this adjustment adversely affected the stability of the retrieval process. The oil volume was gradually reduced until reaching 14.6 mL, under the condition that the ferrofluid could be easily retrieved using a magnet bar for final collection (Figure 3(a)). Subsequently, in the subsequent experiment, a ferrofluid profile diagram was generated to assess the formation of distinct spiked shapes. The ferrofluid was introduced using a magnet bar from varying distances ranging from 0.5 cm to 2.0 cm. Figure 3(b) depicts the

most optimal ferrofluid profile diagram, displaying a cone shape, which was achieved at a distance of 1.0 cm between the peak of the ferrofluid and the magnet bar.

The FTIR analysis conducted on the sample showed the presence of several prominent peaks, including the carboxyl group peak at 1542 cm^{-1}, C-H bonding peak at 1022 cm^{-1}, CH_2 bonding peak at 2941 cm^{-1}, CH_3 bonding peak at 3461 cm^{-1}, C=C bonding peak at 1255 cm^{-1}, and the Fe-O peak at 597.34 cm^{-1} (Figure 4(a)). The C-H stretching vibration band, ranging from 2916 cm^{-1} to 2925 cm^{-1}, confirmed the existence of palmitic saturated fatty acid within the palm oil, while the symmetric CH_2 stretch indicated the presence of oleic acid (Javed et al. 2018). Moreover, the saturation magnetization (Ms) was measured at 42.46 emu/g, which proved to be comparable to Fe_3O_4 coated with oleic acid at 53.4 emu/g, but notably higher than the values reported in the literature, particularly when employing lubricant-type kerosene at 23.72 emu/g (Phor & Kumar 2019).

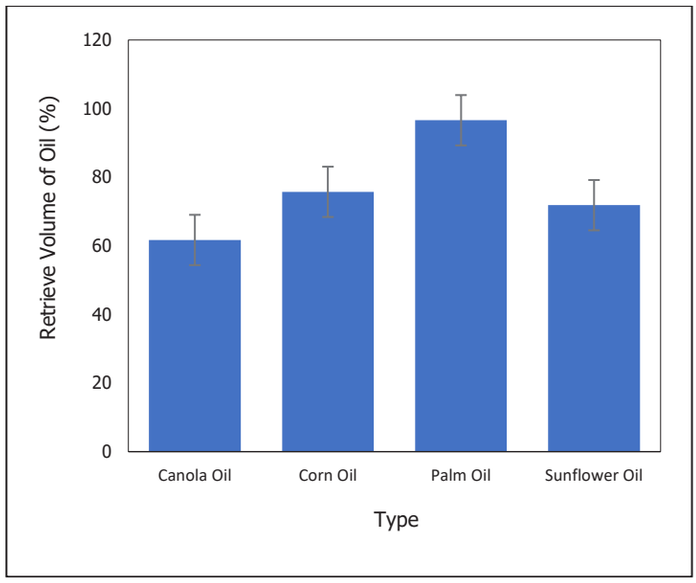

FIGURE 2. Comparison of oil recovery used as ferrofluid

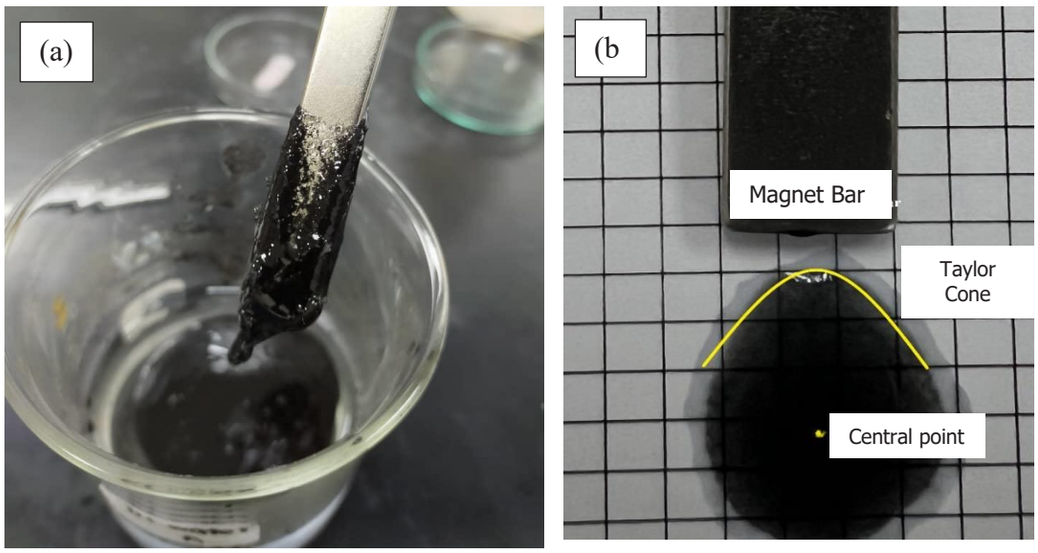

FIGURE 3. (a) Retrieval process ferrofluid using magnet rod and (b) ferrofluid cone diagram

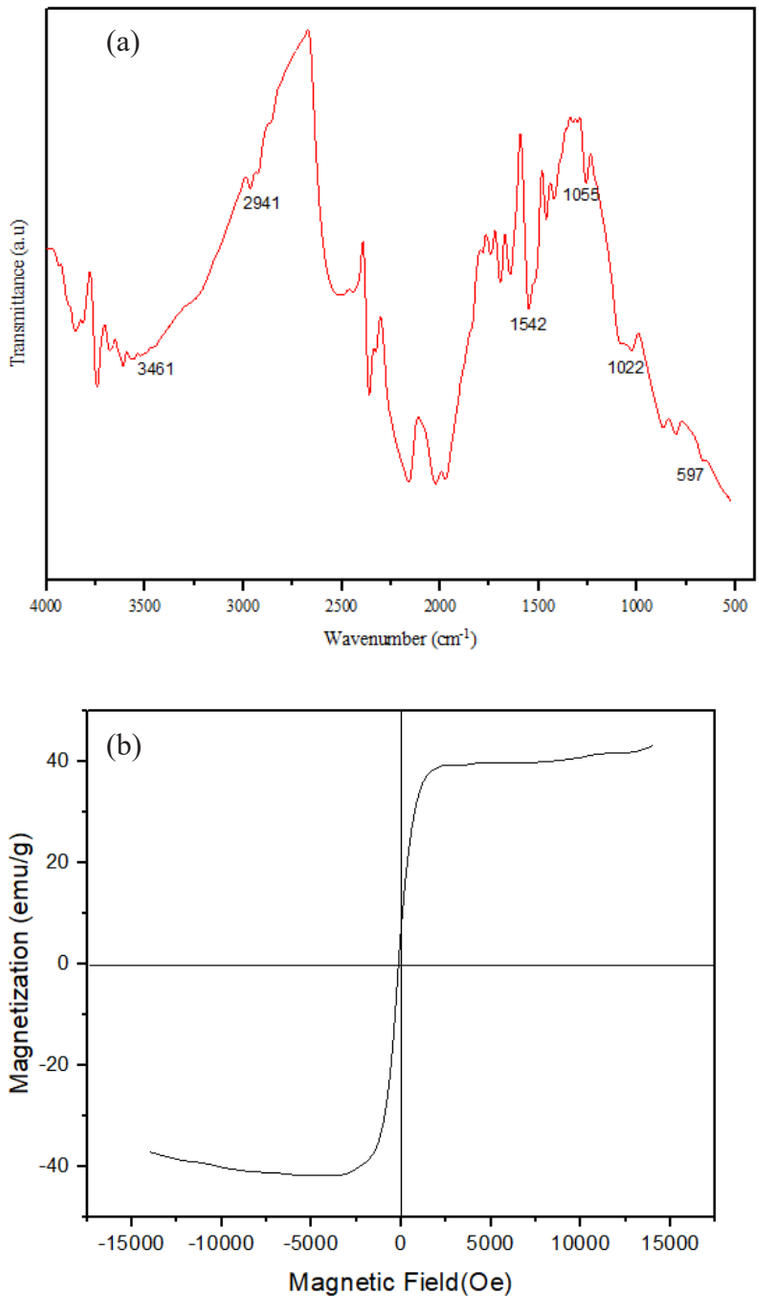

FIGURE 4. (a) FTIR spectra and (b) VSM graph for formulated oil based ferrofluid

SCREENING PARAMETERS

Figure 5 presents the Pareto chart, offering a visual representation of the analysis. In order to assess the impact of each variable on the removal procedure, a t-statistic test was performed, and a standard effect was estimated. Notably, five variables, namely the weight of oil, weight of magnetite nanoparticles, ionic strength effect, stirring rate, and contact time, exhibited

effect estimates (absolute value) exceeding 0.05. This indicates that these variables significantly influenced the removal efficiency and should be further optimized for subsequent analysis, while the pH value of the water remained constant throughout the study. The length of the bars in the Pareto chart corresponded proportionally to the absolute value of the standard effects, with positive or negative signs indicating enhancements or reductions in the response (removal %) as the variable transitioned from the lowest to the highest set level, as discussed by Asadollahzadeh et al. (2014). The wide range of micro-PS removal rates, spanning from 56.85% to 114.75%, emphasized the need to optimize the experimental conditions (Table 4). Notably, the findings of the study underscored the significant influence of the kinetic effect on the removal procedure.

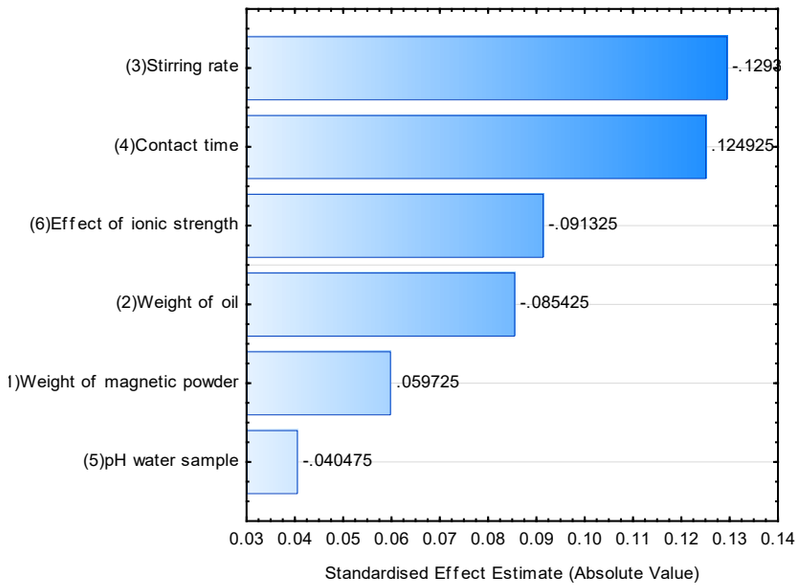

FIGURE 5. Pareto charts of the main effects obtained from a Placket-Burman design

TABLE 4. Removal efficiency obtained from a screening experiment

Run order	Weight of magnetite nanoparticles (g)	Volume of oil (mL)	Stirring rate (rpm)	Contact time (min)	pH of water sample	Effect of ionic strength (g/L)	Removal (%)
1	0.1	12.5	200	10	8	15	88.77
7	0.2	25	200	10	6	5	97.38
2	0.1	12.5	400	10	6	5	97.47
5	0.2	12.5	200	5	6	15	114.75
6	0.2	12.5	400	5	8	5	76.45
8	0.2	25	400	10	8	15	81.72
4	0.1	25	400	5	6	15	56.85
3	0.1	25	200	5	8	5	85.32

In the subsequent experiment, the pH value variables of the water samples were set within the range of pH 6 to pH 6.5. Although their impact was found to be minimal in the present study, it is important to note that this mimic condition design could potentially be applicable when working with real marine samples.

OPTIMIZATION REMOVAL PROCEDURE

The experimental results for micro-PS removal using ferrofluid are presented in Table 5. All model terms were included in the ANOVA test without requiring any data transformation. Statistical significance at a 95% confidence level was determined by p-values below 0.05 in the ANOVA test table. Notably, the ANOVA test showed that the F-value of the model (F_{model} = 20.18) significantly exceeded the tabular F-value at similar degrees of freedom ($F_{0.05\ (4,\ 17)}$ = 2.96), indicating highly significant treatment differences. Detailed results of the ANOVA test can be found in Table 6.

The relationship between the five independent variables and the response (percentage micro-PS removal) was defined by a quadratic polynomial equation, which was obtained from the experimental results and expressed in coded units. The equation derived from the conducted experiments can be expressed as a second-order polynomial equation.

$$Y = 82.71 - 1.15L_1 - 6.53L_2 - 1.88L_3 - 4.48L_4 + 10.11Q_1 \quad (2)$$
$$+7.83Q_2 + 0.99Q_3 + 5.28Q_4 + 4.06L_1L_2 - 6.48L_1L_3$$
$$+2.59L_1L_4 - 13.17L_2L_3 - 17.61L_2L_4 - 10.49\ L_3L_4$$

TABLE 5. The conditions of the central composite design experiments and the responses (% removal)

Run order	Contact time (min)	Stirring rate (rpm)	Ionic strength (g/L)	Volume of oil (mL)	Removal (%)
1	10	400	15	6	100.96
2	10	400	5	6	114.41
3	10	200	15	13	104.25
4	5	400	5	13	93.41
5	10	200	5	13	112.29
6	5	200	15	6	113.28
7	5	400	15	13	71.98
8	5	200	5	6	87.43
9	3	300	8	9	88.87
10	12	300	8	9	92.41
11	8	132	8	9	87.48
12	8	468	8	9	87.34
13	8	300	-1	9	83.19
14	8	300	16	9	72.19
15	8	300	8	4	83.00
16	8	300	8	15	84.62
17 (C)	8	300	8	9	91.40
18 (C)	8	300	8	9	91.66

The constructed model encompassed four primary effects (L_{1-4}), four two-factor effects (Q_1-$_4$), and six curvature effects (L_XLy), with an intercept value of 82.71. The model parameters were optimized through iterative processes to effectively capture and represent the data. Model validation yielded a coefficient of determination (R^2) of 0.966 and an adjusted R^2 (adj-R^2) of 0.907. While R^2 increased with the inclusion of additional model terms (variables), adj-R^2 took into account the reduction in response variability achieved by incorporating the predictor variables into the model.

The optimization graph provides a visual representation of the predicted conditions for the optimal point and the desirability of the predictions. Each plot within the graph illustrates the influence of a specific variable on micro-PS removal. In Figure 6, the red lines indicate the significant optimum values for each variable. Profiling the response desirability involved assigning predicted values on a scale ranging from 0.0 to 1.0 for each dependent variable. In this study, an overall desirability of 0.95 was achieved, which is considered good within the studied range.

TABLE 6. Analysis of variance (ANOVA) for the proposed model

	SS	Df	MS	F	P
Contact time (min) (1L)	1.602	1	1.601	47.39	0.091
Contact time (min) (1Q)	298.999	1	298.999	8846.12	0.006
Stirring rate (2L)	51.211	1	51.211	1515.13	0.016
Stirring rate (2Q)	179.187	1	179.187	5301.39	0.008
Ionic strength (3L)	11.681	1	11.681	345.61	0.034
Ionic strength (3Q)	3.588	1	3.587	106.15	0.061
Volume oil (4L)	24.084	1	24.084	712.55	0.023
Volume oil (4Q)	81.610	1	81.610	2414.50	0.012
1L by 2L	12.379	1	12.378	366.24	0.033
1L by 3L	83.916	1	83.916	2482.72	0.012
1L by 4L	5.050	1	5.049	149.40	0.051
2L by 3L	347.030	1	347.029	10267.15	0.006
2L by 4L	232.677	1	232.677	6883.93	0.007
3L by 4L	219.992	1	219.992	6508.64	0.007
Lack of fit	749.437	2	374.718	11086.35	0.006
Pure error	0.034	1	0.033		
Total SS	2677.885	17			

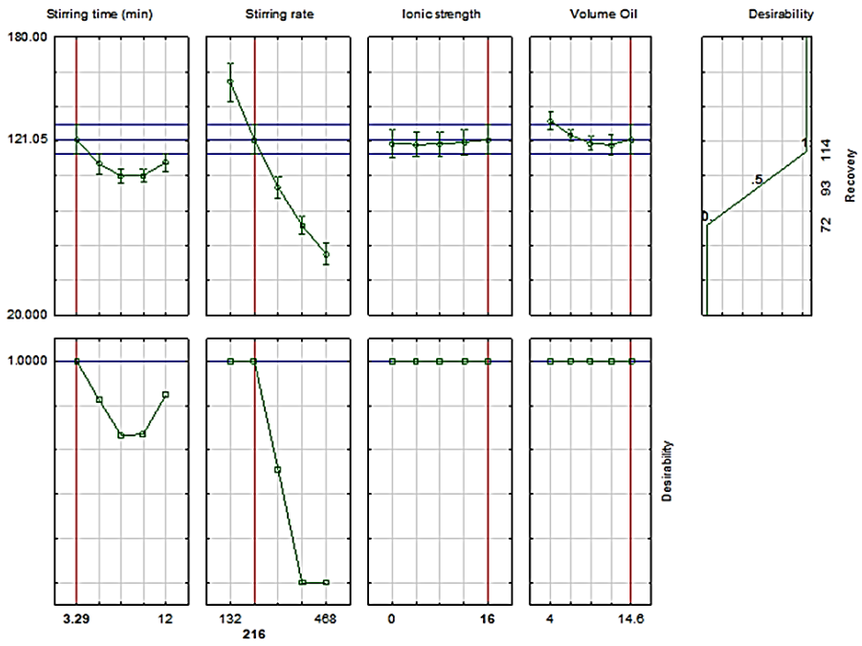

FIGURE 6. Profiles for predicted values and desirability function for the optimum model

The 3D response surfaces and contour plots of the model are illustrated in Figures 7 to 9. These plots showcase the mapping of responses against two experimental variables, while the remaining variables are kept constant at their central level. Among the variables, the volume of the carrier liquid plays a critical role in optimizing the structural stability of the ferrofluid. This stability is crucial in preventing the settling or aggregation of magnetic nanoparticles within the ferrofluid. Maintaining stability ensures that the nanoparticles do not clump together or form larger aggregates, which would impede their ability to effectively attach to and agglomerate with micro-PS. In the aqueous phase, the ferrofluid tended to disperse across a larger surface area. This dispersion allowed for a reduced contact time with the micro-PS, thereby enhancing the kinetic effects. The absence of nanoparticle aggregation can be attributed to the presence of a surfactant layer, such as oleic acid, covering the nanoparticles. Fatty acids, like oleic acid, are commonly utilized as stabilizers for hydrocarbons, aiding in the prevention of aggregation.

The longevity of the ferrofluid was determined by the good stability of the nanoparticle suspension. This stability was influenced by two opposing forces: repulsive forces (such as Brownian motion, steric forces, and electrostatic forces) and attractive forces (such as Van der Waals and dipolar interactions). However, when an external magnetic field was applied, the magnetic particles in the ferrofluid became magnetized into magnetic dipoles. As a result, they attracted each other under the influence of the external magnetic field, aligning themselves in the direction of the magnetic field (Wang et al. 2022). In Figure 7, the 3D relationship between the volume of oil (in mL) and the contact time (in min) is depicted. The figure demonstrates an increasing trend in micro-PS removal when the ferrofluid was exposed for a longer duration in the aqueous phase, ranging from 8 min to 12 min. The volume of palm oil, serving as the carrier liquid, contributed to a significant 27.19% enhancement in micro-PS removal.

The stirring rate implemented in the aqueous phase played a crucial role in dispersing the ferrofluids in water and capturing buoyant micro-PS particles at the water surface. To maximize the contact area between the ferrofluid and micro-PS, it was recommended to lower the stirring speed, allowing for the maintenance of a layered ferrofluid on the top surface. Adequate stirring facilitated the formation of larger agglomerates by increasing the collision frequency between nanoparticles

and micro-PS, leading to more effective binding and agglomeration. In reference to Figure 8, the relationship between stirring rate and contact time could be optimized in two ways: firstly, by lowering the speed to a range of 100 rpm to 150 rpm while extending the duration of ferrofluid exposure to 9 min to 11 min; alternatively, by reducing the exposure time to a range of 2 min to 4 min and increasing the stirring speed to a range of 400 rpm to 500 rpm. It is worth noting that a significant increase in stirring speed was less favorable, as it caused the oil layer to break into tiny droplets, complicating the retrieval process. Both variables collectively contributed to a removal efficiency of 1.34%, which was lower than the calculated value for individual contributions: stirring rate (57.8%) and contact time (1.80%), respectively.

The presence of ionic strength played a significant role in increasing the density of water, thereby facilitating the easy floatation and removal of both micro-PS and

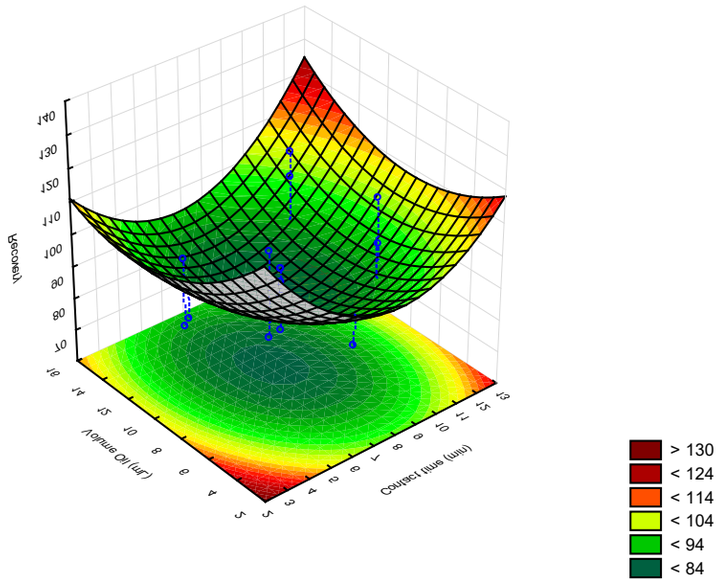

FIGURE 7. 3D relationship between contact time (min) *vs* volume oil (mL)

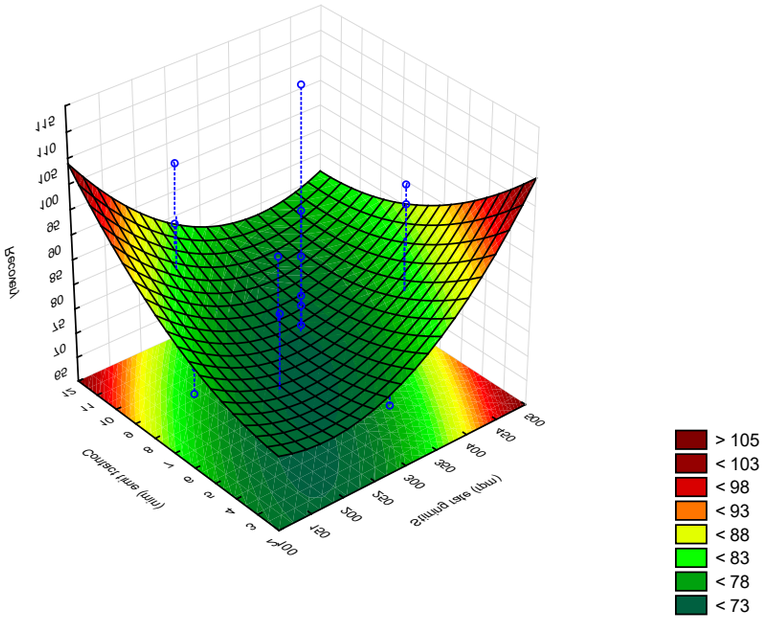

FIGURE 8. 3D relationship between contact time (min) *vs* stirring rate (rpm)

ferrofluids through the application of magnets. An increase in ionic strength led to the formation of a double electric layer around the nanoparticles, reducing the strength of attractive forces between them and subsequently decreasing repulsion in the colloidal phase. The aggregation of magnetite nanoparticles was further accelerated by the stirring rate and duration (Oda & Kitamoto 2017). Another aspect to consider is the addition of salts to the aqueous solution, which enhanced its density and surface charge. When micro-PS were immersed in a high-density solution due to increased ionic strength, their buoyancy was enhanced. The greater the disparity between the density of the micro-PS and the surrounding solution, the more likely they were to float. The surface charge of micro-PS increased their tendency to repel each other, thereby remaining buoyant. Under acidic conditions (pH 6), the surface of polystyrene microplastics became positively charged due to the protonation of functional groups (Wang et al. 2022). Consequently, a significant amount of ferrofluids could be easily collected using an external magnet, as depicted in Figure 9. The percentage removal exhibited an increasing trend ranging from 2 to 16 g/L. In the removal system, the addition of NaCl contributed to an efficiency enhancement of up to 13.18%.

The highest removal efficiency of micro-PS from water, reaching 93%, was achieved under the optimal conditions of 14.6 mL volume of oil, 0.1 g weight of magnetite, 216 rpm stirring rate, 3.29 min contact time, pH 6 value for the water sample, and an ionic strength effect of 16 g/L. These recommended conditions yielded the most effective removal of micro-PS contaminants from the water system.

FEASIBILITY TEST

To validate the proposed model, additional experiments were conducted under the given optimal conditions, with a total of five replicates (n = 5). The results demonstrated a micro-PS removal efficiency of 91.09 ± 0.99%, with approximately 83.05% of the ferrofluid successfully collected. However, the reusability test showed a gradual decrease in the amount of ferrofluid collected, reaching 73.40% after five cycles. The comparison between the predicted model values and the actual experimental values did not yield any significant differences ($p > 0.05$), indicating good agreement.

Furthermore, an analysis using AGREEprep showed that the micro-PS removal procedure aligned with several green analytical criteria. It excelled in aspects such as (1) *in situ* sample preparation, (5) minimizing the usage of samples, chemicals, and materials, (8) achieving minimum energy consumption, and (9) employing the greenest approach in post-sample preparation configuration for analysis. However, there were areas identified for improvement, including (3) aiming for maximum usage of sustainable, reusable, and renewable materials, (4) minimizing waste generation, (6) maximizing simultaneous sample preparation, and (7) aiming for automation in sample preparation. To visually depict the degree of compatibility with the green analytical criteria, Figure 10 presents a pictogram that helps illustrate the level of adherence to these criteria.

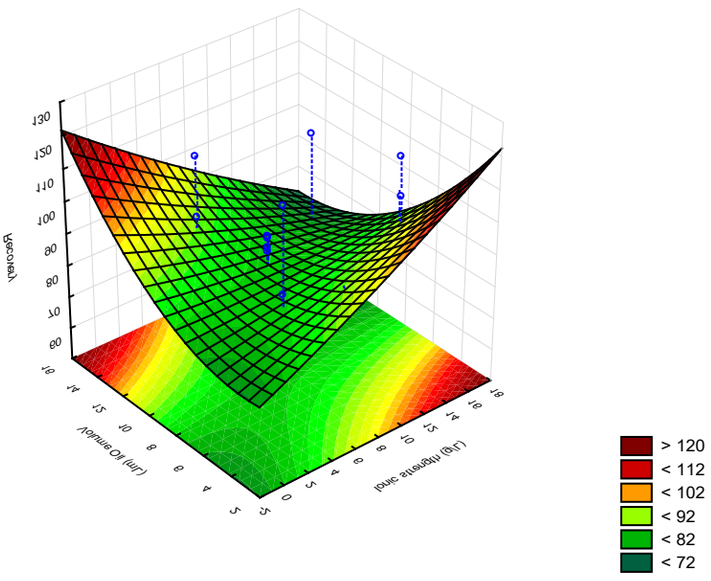

FIGURE 9. 3D relationship between volume oil (mL) *vs* ionic strength (g/L)

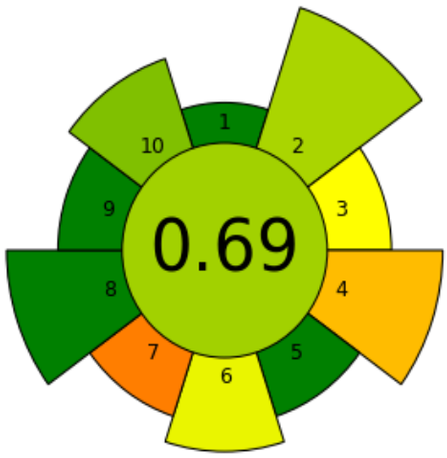

FIGURE 10. The results of AGREEprep assessment of micro-PS removal procedure

CONCLUSIONS

The formulation of ferrofluids using palm oil as the carrier liquid, in combination with magnetite nanoparticles, was explored in this study. The high concentration of palmitic acid in palm oil acted as an effective surfactant and stabilizer for the ferrofluids. The central composite design revealed that stirring rate, contact time, volume of oil, and ionic strength had significant impacts on the removal of micro-PS, while the weight of magnetite and pH value of the water sample had comparatively lesser influence. The proposed model indicated that the optimal conditions could achieve a removal efficiency of up to 93%, which was in line with the actual experiment where the highest percentage removal was observed at 91.09 ± 0.99%. The pictogram generated from AGREEprep displayed a light green color, highlighting the environmentally friendly nature of the ferrofluid-based sample preparation methodology. Moreover, this method holds potential for removing other types of microplastic pollutants, such as microfibers, fragments, and films, making it applicable to a broader range of environmental concerns.

REFERENCES

Amelia, T.S.M., Khalik, W.M.A.W.M., Ong, M.C., Shao, Y.T., Pan, H.J. & Bhubalan, K. 2021. Marine microplastics as vectors of major ocean pollutants and its hazards to the marine ecosystem and humans. *Progress in Earth and Planetary Science* 8(1): 1-26.

Asadollahzadeh, M., Tavakoli, H., Torab-Mostaedi, M., Hosseini, G. & Hemmati, A. 2014. Response surface methodology based on central composite design as a chemometric tool for optimization of dispersive-solidification liquid–liquid microextraction for speciation of inorganic arsenic in environmental water samples. *Talanta* 123: 25-31.

Bezerra, M.A., Santelli, R.E., Oliveira, E.P., Villar, L.S. & Escaleira, L.A. 2008. Response surface methodology (RSM) as a tool for optimization in analytical chemistry. *Talanta* 76(5): 965-977.

Chen, F., Liu, X., Li, Z., Yan, S., Fu, H. & Yan, Z. 2021. Investigation of the rheological properties of Zn-ferrite/perfluoropolyether oil-based ferrofluids. *Nanomaterials* 11(10): 2653.

Choong, W.S., Hadibarata, T., Yuniarto, A., Tang, K.H.D., Abdullah, F., Syafrudin, M., Al Farraj, D.A. & Al-Mohaimeed, A.M. 2021. Characterization of microplastics in the water and sediment of Baram River estuary, Borneo Island. *Marine Pollution Bulletin* 172: 112880.

Davudabadi Farahani, M., Shemirani, F., Fasih Ramandi, N. & Gharehbaghi, M. 2015. Ionic liquid as a ferrofluid carrier for dispersive solid phase extraction of copper from food samples. *Food Analytical Methods* 8(8): 1979-1989.

Deng, Y., Zhang, Y., Lemos, B. & Ren, H. 2017. Tissue accumulation of microplastics in mice and biomarker responses suggest widespread health risks of exposure. *Scientific Reports* 7(1): 46687.

Hamzah, S., Ying, L.Y., Azmi, A.A.A.R., Razali, N.A., Hairom, N.H.H., Mohamad, N.A. & Harun, M.H.C. 2021. Synthesis, characterisation and evaluation on the performance of ferrofluid for microplastic removal from synthetic and actual wastewater. *Journal of Environmental Chemical Engineering* 9(5): 105894.

Hanrahan, G. & Lu, K. 2006. Application of factorial and response surface methodology in modern experimental design and optimization. *Critical Reviews in Analytical Chemistry* 36(3-4): 141-151.

Henriques, K. 2022. Analysis of the microplastic removal efficiency of synthesized ferrofluids and the development of an automated prototype for aquatic environments. *The Columbia Junior Science Journal* 2022: 1-5.

Hüffer, T., Weniger, A.K. & Hofmann, T. 2018. Sorption of organic compounds by aged polystyrene microplastic particles. *Environmental Pollution* 236: 218-225.

Issac, M.N. & Kandasubramanian, B. 2021. Effect of microplastics in water and aquatic systems. *Environmental Science and Pollution Research* 28(16): 19544-19562.

Javed, M., Shaik, A.H., Khan, T.A., Imran, M., Aziz, A., Ansari, A.R. & Chandan, M.R. 2018. Synthesis of stable waste palm oil based CuO nanofluid for heat transfer applications. *Heat and Mass Transfer* 54: 3739-3745.

Joseph, A. & Mathew, S. 2014. Ferrofluids: Synthetic strategies, stabilization, physicochemical features, characterization, and applications. *ChemPlusChem* 79(10): 1382-1420.

Kadakia, K. 2012. Removal of arsenic contamination from water using magnetite nanoparticles. *The National High School Journal* 2012: 1-7.

Khalik, W.M.A.W.M., Ibrahim, Y.S., Anuar, S.T., Govindasamy, S. & Baharuddin, N.F. 2018. Microplastics analysis in Malaysian marine waters: A field study of Kuala Nerus and Kuantan. *Marine Pollution Bulletin* 135: 451-457.

Lapointe, M., Farner, J.M., Hernandez, L.M. & Tufenkji, N. 2020. Understanding and improving microplastic removal during water treatment: Impact of coagulation and flocculation. *Environmental Science & Technology* 54(14): 8719-8727.

Li, J., Huang, W., Xu, Y., Jin, A., Zhang, D. & Zhang, C. 2020. Microplastics in sediment cores as indicators of temporal trends in microplastic pollution in Andong salt marsh, Hangzhou Bay, China. *Regional Studies in Marine Science* 35: 101149.

Li, L.C. & Li, I.K. 2021. Study of ferrofluid and magnetic fields. *Proceedings of the International Conference on Industrial Engineering and Operations Management*. pp. 6751-6761.

Liu, H., Zhou, X., Ding, W., Zhang, Z., Nghiem, L.D., Sun, J. & Wang, Q. 2019. Do microplastics affect biological wastewater treatment performance? Implications from bacterial activity experiments. *ACS Sustainable Chemistry & Engineering* 7(24): 20097-20101.

Ma, B., Xue, W., Hu, C., Liu, H., Qu, J. & Li, L. 2019. Characteristics of microplastic removal via coagulation and ultrafiltration during drinking water treatment. *Chemical Engineering Journal* 359: 159-167.

Ma, M., Liu, S., Su, M., Wang, C., Ying, Z., Huo, M., Lin, Y. & Yang, W. 2022. Spatial distribution and potential sources of microplastics in the Songhua River flowing through urban centers in Northeast China. *Environmental Pollution* 292: 118384.

Martinez, L. & Kim, B. 2020. Removal of microplastics in water using oil-based ferrofluid solution. New Jersey City University.

Mušović, J., Vraneš, M., Papović, S., Gadžurić, S., Ražić, S. & Trtić-Petrović, T. 2023. Greener sample preparation method for direct determination of Cd (II) and Pb (II) in river sediment based on an aqueous biphasic system with functionalized ionic liquids. *Journal of Molecular Liquids* 369: 120974.

Nabeel Rashin, M., Kutty, R.G. & Hemalatha, J. 2014. Novel coconut oil based magnetite nanofluid as an ecofriendly oil spill remover. *Industrial & Engineering Chemistry Research* 53(40): 15725-15730.

Nayebi, R. & Shemirani, F. 2021. Ferrofluids-based microextraction systems to process organic and inorganic targets: The state-of-the-art advances and applications. *TrAC Trends in Analytical Chemistry* 138: 116232.

Oda, S. & Kitamoto, Y. 2017. Relationship between ion concentration of ferrofluid and response signals of magnetic nanoparticles against ac magnetic fields. *AIP Advances* 7(5): 056729.

Oehlsen, O., Cervantes-Ramírez, S.I., Cervantes-Avilés, P. & Medina-Velo, I.A. 2022. Approaches on ferrofluid synthesis and applications: Current status and future perspectives. *ACS Omega* 7(4): 3134-3150.

Peñalver, R., Costa-Gómez, I., Arroyo-Manzanares, N., Moreno, J.M., López-García, I., Moreno-Grau, S. & Córdoba, M.H. 2021. Assessing the level of airborne polystyrene microplastics using thermogravimetry-mass spectrometry: Results for an agricultural area. *Science of The Total Environment* 787: 147656.

Phor, L. & Kumar, V. 2019. Self-cooling by ferrofluid in magnetic field. *SN Applied Sciences* 1: 1-9.

Pizzichetti, A.R.P., Pablos, C., Álvarez-Fernández, C., Reynolds, K., Stanley, S. & Marugán, J. 2021. Evaluation of membranes performance for microplastic removal in a simple and low-cost filtration system. *Case Studies in Chemical and Environmental Engineering* 3: 100075.

Poerio, T., Piacentini, E. & Mazzei, R. 2019. Membrane processes for microplastic removal. *Molecules* 24(22): 4148.

Pramanik, B.K., Pramanik, S.K. & Monira, S. 2021. Understanding the fragmentation of microplastics into nano-plastics and removal of nano/microplastics from wastewater using membrane, air flotation and nano-ferrofluid processes. *Chemosphere* 282: 131053.

Rajala, K., Grönfors, O., Hesampour, M. & Mikola, A. 2020. Removal of microplastics from secondary wastewater treatment plant effluent by coagulation/flocculation with iron, aluminum and polyamine-based chemicals. *Water Research* 183: 116045.

Scherer, C. & Figueiredo Neto, A.M. 2005. Ferrofluids: Properties and applications. *Brazilian Journal of Physics* 35: 718-727.

Shi, X., Chen, Z., Liu, X., Wei, W. & Ni, B.J. 2022. The photochemical behaviors of microplastics through the lens of reactive oxygen species: Photolysis mechanisms and enhancing photo-transformation of pollutants. *Science of The Total Environment* 2022: 157498.

Shi, Z.G., Zhang, Y. & Lee, H.K. 2010. Ferrofluid-based liquid-phase microextraction. *Journal of Chromatography A* 1217(47): 7311-7315.

Siipola, V., Pflugmacher, S., Romar, H., Wendling, L. & Koukkari, P. 2020. Low-cost biochar adsorbents for water purification including microplastics removal. *Applied Sciences* 10(3): 788.

Sun, J., Dai, X., Wang, Q., van Loosdrecht, M.C. & Ni, B.J. 2019. Microplastics in wastewater treatment plants: Detection, occurrence and removal. *Water Research* 152: 21-37.

Tofa, T.S., Kunjali, K.L., Paul, S. & Dutta, J. 2019. Visible light photocatalytic degradation of microplastic residues with zinc oxide nanorods. *Environmental Chemistry Letters* 17: 1341-1346.

Wang, H., Meng, Y., Li, Z., Dong, J. & Cui, H. 2022. Steady-state and dynamic rheological properties of a mineral oil-based ferrofluid. *Magnetochemistry* 8(9): 100.

Wenzel, M., Fischer, B., Renner, G., Schoettl, J., Wolf, C., Schram, J., Schmidt, T.C. & Tuerk, J. 2022. Efficient and sustainable microplastics analysis for environmental samples using flotation for sample pre-treatment. *Green Analytical Chemistry* 3: 100044.

Wojnowski, W., Tobiszewski, M., Pena-Pereira, F. & Psillakis, E. 2022. AGREEprep–Analytical greenness metric for sample preparation. *TrAC Trends in Analytical Chemistry* 149: 116553.

Yap, K.Y. & Tan, M.C. 2021. Oil adsorption onto different types of microplastic in synthetic seawater. *Environmental Technology & Innovation* 24: 101994.

*Corresponding author; email: wan.afiq@umt.edu.my